JACS
JOURNAL OF THE AMERICAN CHEMICAL SOCIETY

Article

pubs.acs.org/JACS

Membrane Orientation of $G\alpha_i\beta_1\gamma_2$ and $G\beta_1\gamma_2$ Determined via Combined Vibrational Spectroscopic Studies

Pei Yang,[†] Andrew Boughton,[†] Kristoff T. Homan,[‡] John J. G. Tesmer,*[,‡] and Zhan Chen*[,†]

[†]Department of Chemistry, University of Michigan, 930 North University Avenue, Ann Arbor, Michigan 48109, United States

[‡]Departments of Pharmacology and Biological Chemistry, Life Sciences Institute, University of Michigan, Ann Arbor, Michigan 48109, United States

Supporting Information

ABSTRACT: The manner in which the heterotrimeric G protein complexes $G\beta_1\gamma_2$ and $G\alpha_i\beta_1\gamma_2$ interact with membranes is likely related to their biological function. We combined complementary measurements from sum frequency generation (SFG) vibrational and attenuated total reflectance Fourier transform infrared (ATR-FTIR) spectroscopy to determine the possible membrane orientations of $G\beta_1\gamma_2$ and the $G\alpha_i\beta_1\gamma_2$ heterotrimer more precisely than could be achieved using SFG alone. The most likely orientations of $G\beta_1\gamma_2$ and the $G\alpha_i\beta_1\gamma_2$ heterotrimer were both determined to fall within a similar narrow range of twist and tilt angles, suggesting that $G\beta_1\gamma_2$ may bind to $G\alpha_i$ without a significant change in orientation. This "basal" orientation seems to depend primarily on the geranylgeranylated C-terminus of $G\gamma_2$ along with basic residues at the N-terminus of $G\alpha_i$, and suggests that activated G protein-coupled receptors (GPCRs) must reorient G protein heterotrimers at lipid bilayers to catalyze nucleotide exchange. The innovative methodologies developed in this paper can be widely applied to study the membrane orientation of other proteins *in situ*.

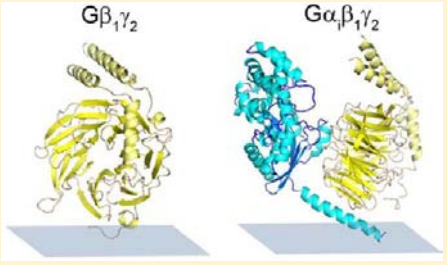

INTRODUCTION

The orientation of peptides and proteins at interfaces plays a critical role in many research areas and applications such as biocompatibility, marine antifouling coatings, biosensors and biochips, membrane protein functions, and antimicrobial activity and selectivity.[1−8] However, the orientation of peptides and proteins at solid/liquid interfaces is difficult to analyze, particularly *in situ* and with molecular level detail. In recent years, we have demonstrated that sum frequency generation (SFG) vibrational spectroscopy can be used to determine the interfacial orientation of simple peptides that adopt various secondary structures (such as α-helices, 3_{10}-helices, and antiparallel β-sheets).[9−20] We have also shown that SFG can be used to study the orientation of α-helical domains of interfacial proteins.[21,22] However, for proteins with more complicated structures, a single measurement yields a broad range of likely orientations. We hypothesize that complementary measurements obtained from attenuated total reflectance−Fourier transform infrared (ATR-FTIR) spectroscopy[10,23,24] can be combined with SFG data to obtain a more precise and detailed picture of how a molecule orients at an interface. In ATR-FTIR, a total internal reflection scheme is used to produce reasonable surface sensitivity (on the order of hundreds of nanometers to micrometers) based on the penetration depth of the evanescent wave into the sample. ATR-FTIR has been used to study the orientation of a wide variety of α-helical[25−27] and β-sheet[28,29] peptides, but because ATR-FTIR by itself only produces a limited number of measurements, studies of larger proteins[30−34] have typically relied on the assumption that all secondary structural elements are roughly aligned in the protein (e.g., proteins with a β-barrel structure). However, the fold of most proteins does not follow this assumption. In this work, we demonstrate that the orientation of proteins with more complex folds (such as the $G\alpha_i\beta_1\gamma_2$ heterotrimer and $G\beta_1\gamma_2$ subunit) can be achieved by a combination of SFG and ATR-FTIR measurements.

Heterotrimeric G proteins ($G\alpha\beta\gamma$) comprise three subunits ($G\alpha$, $G\beta$, and $G\gamma$), with $G\beta$ and $G\gamma$ forming a constitutive heterodimer ($G\beta\gamma$).[35] When $G\alpha$ is bound to GDP, it forms an inactive complex with $G\beta\gamma$ that serves as the substrate for activated G protein-coupled receptors (GPCRs), which catalyze the release of GDP and the binding of GTP to $G\alpha$. Upon activation of the GPCR, the $G\alpha$·GTP and $G\beta\gamma$ subunits are released and can independently interact with and regulate additional proteins that propagate signals within the cell.[36] The $G\beta\gamma$ subunit is essential for coupling the heterotrimeric G protein to activated GPCRs, although it does not appear to make direct interactions with the receptor.[37] $G\beta\gamma$ facilitates membrane localization of the $G\alpha\beta\gamma$ heterotrimer via C-terminal prenylation of the $G\gamma$ subunit, but it may also allosterically promote nucleotide exchange or help dictate a particular orientation of the heterotrimer that is more optimal for engaging GPCRs. Free $G\beta\gamma$ subunits also play a major role in recruiting G protein-coupled receptor kinase 2 (GRK2) to the cell membrane.[38−40] In previous work, sum frequency

Received: November 27, 2012
Published: March 5, 2013

   dx.doi.org/10.1021/ja3116026 | J. Am. Chem. Soc. 2013, 135, 5044−5051

generation (SFG) studies were used to determine possible orientations of GRK2-G$\beta_1\gamma_2$ and G$\beta_1\gamma_2$, and we demonstrated that G$\beta_1\gamma_2$ changes its orientation with respect to the membrane upon binding to GRK2.[41] However, the limited number of direct experimental measurements hindered attempts to narrow the molecular orientation to ranges of twist and tilt angles (defined in Figure 1) smaller than 20−30°.

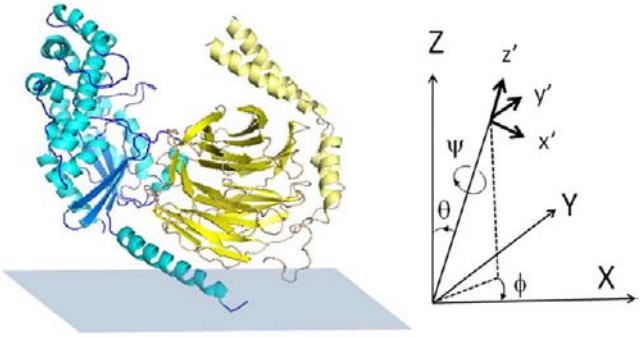

Figure 1. The G$\alpha_i\beta_1\gamma_2$ heterotrimer and definition of twist (ψ), tilt (θ) and azimuthal (ϕ) angles which rotate the protein from the molecular (x', y', z') to the macroscopic (X, Y, Z) coordinate system. G$\beta_1\gamma_2$ is shown in yellow, and Gα_i is shown in cyan. An approximate membrane plane (defined to be consistent with previous studies of GRK2-G$\beta_1\gamma_2$),[41] is shown as a blue rectangle, and lies parallel to the X−Y plane. The G$\alpha_i\beta_1\gamma_2$ heterotrimer is depicted in the reference orientation (ψ = 0°, θ = 0°, ϕ = 0°) used as a starting point for data analysis. In our calculations, the molecule is rotated using an Euler rotation scheme according to three angles: first twist (ψ) then tilt (θ), and finally azimuthal (ϕ).

Herein, we used a combination of SFG and ATR-FTIR to determine the orientation of G$\beta_1\gamma_2$ and the G$\alpha_i\beta_1\gamma_2$ heterotrimer. By combining orientation information from multiple spectroscopic measurements of several related proteins with common binding partners, we show it is possible to more accurately determine membrane orientations, and ascertain whether the formation of higher order complexes induces changes in orientation that could have biological consequences.

MATERIALS AND METHODS

Protein Samples. Nonmysristoylated rat Gα_{i1} and myristoylated Gα_{i1} (myr-Gα_{i1}) were expressed in bacteria and bovine G$\beta_1\gamma_2$ was expressed in High5 insect cells and the proteins were purified as previously described,[42,43] and frozen in liquid nitrogen until used. The G$\alpha_i\beta_1\gamma_2$ heterotrimer was either formed by sequential addition of Gα_{i1} to G$\beta_1\gamma_2$ in the SFG sample cell, or by mixing them in a 1:1 ratio followed by purification of the complex on a Superdex S200 gel filtration column equilibrated with 20 mM HEPES (pH 8.0), 50 mM NaCl, and 5 mM dithiothreitol (DTT). This buffer mixture was also used as the liquid subphase for the lipid bilayer in SFG and ATR-FTIR studies.

SFG Spectroscopy. Second-order nonlinear optical spectroscopy has been widely used to study surfaces and interfaces and the relevant theoretical background has been extensively reported.[44−78] The design of our SFG spectrometer is described elsewhere.[45] SFG spectra from interfacial protein samples were collected at room temperature (24 °C) in a near total internal reflection geometry for the ssp and ppp polarization combinations of the sum frequency, visible, and infrared beams.[46] Planar supported lipid bilayers (PSLBs) were prepared on clean right-angle CaF_2 prisms (Altos Photonics, Bozeman MT) using the Langmuir−Blodgett/Langmuir−Schaefer method, as described previously.[41] A 9:1 mixture of 1-palmitoyl-2-oleoyl-*sn*-glycero-3-phosphocholine (POPC) and 1-palmitoyl-2-oleoyl-*sn*-glycero-3-phosphoglycerol (POPG) lipids was used. The lipids were purchased in a chloroform solution (Avanti Polar Lipids, Inc.), and mixed to produce the desired composition. Following equilibration of the bilayer, the aqueous subphase was flushed three times with fresh buffer to remove excess lipids. Samples of the G proteins to be studied were then injected into the aqueous subphase to a final concentration of 336 nM, and allowed to diffuse to the lipid bilayer over the course of 1 h, during which time the time-dependent SFG spectral intensity at 1655 cm^{-1} was monitored. The proteins studied are peripheral (rather than integral) membrane proteins, and thus, no portion of the G proteins used in these experiments spans the lipid bilayer. Following equilibration, SFG spectra in the ppp and ssp polarization combinations were collected from the proteins associated with the lipid bilayer. More details can be found in the Supporting Information and previous publications.[9,41]

ATR-FTIR Spectroscopy. Lipid bilayers of the same composition as above were prepared on clean ZnSe substrates (Specac, U.K.) for ATR-FTIR experiments. Because the vibrational signal of the water O−H bending mode overlaps with the protein amide I signal, we used D_2O in the buffer subphase in the ATR-FTIR experiments. Even so, strong O−H bending signal was observed from the water layer between the ATR crystal and the supported lipid bilayer prepared by the Langmuir−Blodgett/Langmuir−Schaefer method. Because it is impractical to use D_2O in the large Langmuir trough for the sample preparation, lipid bilayers for ATR-FTIR were prepared via the vesicle fusion method.[26,27] The vesicles were prepared via extrusion through 100 nm pores (Avanti Polar Lipids) from lipid solutions reconstituted in PBS (pH 7.4) in deuterated water, after the 9:1 POPC:POPG lipid samples were dried under vacuum for 30 min to remove chloroform. The bilayer was allowed to equilibrate for 1 h, after which time excess vesicle solution was removed by flushing thoroughly with fresh deuterated buffer solution. The sample was allowed to equilibrate again for an additional 30 min. Protein samples (in buffer solution with D_2O as the solvent) were injected into the subphase for a target concentration of 336 nM to match the concentration used in SFG experiments, and samples were allowed to equilibrate for 2 h prior to collection of spectra. P and s polarized spectra were collected on a Nicolet Magna IR 550 spectrometer with the ATR accessory. All spectra presented are the average of 128 scans. To reduce interference from water vapor present in the air, the instrument was purged with dry nitrogen prior to use, and spectra were afterward corrected for trace amounts of water vapor using an additional background correction based on the spectrum of pure water vapor in air at 24 °C.[79] The background subtraction and a baseline correction in the amide I region were performed in OMNIC 2.1, after which spectra were fit to a Gaussian line shape using a nonlinear curve fitting algorithm in Origin 8.1. The dichroic ratio R^{ATR} was determined from the ratio of the absorbance of α-helices in the p and s polarizations of the infrared beam.[27,79] Our method of calculating R^{ATR} for a protein with many separate helical segments is described in the Supporting Information.

RESULTS AND DISCUSSION

Orientation of G$\beta_1\gamma_2$. Gγ_2 is lipid modified with a C-terminal hydrophobic geranylgeranyl group that localizes G$\beta_1\gamma_2$ to membranes. Although G$\beta_1\gamma_2$ has been studied previously using SFG,[41,44] the limited number of resulting measurements meant that it was only possible to determine either the tilt angle (by assuming a constant twist angle)[44] or very broad ranges of possible twist and tilt angles.[41] Although G$\beta_1\gamma_2$ contains regions of nonhelical secondary structures (such as β-sheets), SFG amide I signals from G$\beta_1\gamma_2$ were found to be dominated by contributions from α-helices, possibly due to the high symmetry of the β-propeller. In our previous work, by fitting SFG spectra in the ppp and ssp polarization combinations and correcting for differences in the Fresnel coefficients for the two polarizations, it was found that the measured ratio $\chi^{(2)}_{zzz}/\chi^{(2)}_{xxz}$ for the α-helical peak at 1652 cm^{-1} was 2.01 for G$\beta_1\gamma_2$.[41] Unlike SFG, which only detects signals where inversion symmetry is

dx.doi.org/10.1021/ja3116026 | J. Am. Chem. Soc. 2013, 135, 5044−5051

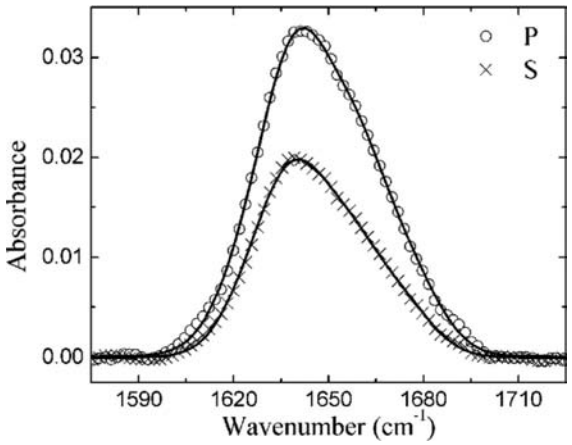

Figure 2. Experimental ATR-FTIR spectra of 336 nM membrane-bound G$\beta_1\gamma_2$ on 9:1 POPC:POPG lipid bilayer for the p and s polarizations. The circles and crosses are experimental data. The solid lines are the fitting results.

broken, ATR-FTIR signals are generated by all secondary structures. Therefore, the ATR-FTIR spectra contained vibrational peaks at 1635, 1643, 1657, and 1671 cm^{-1}, for β-sheet, random coil/disordered structure, α-helix, and β-turn, respectively (see Supporting Information),[27,79] resulting in a broader overall line shape than in SFG (Figure 2). The fitted dichroic ratio R^{ATR} for the α-helical peak was 1.70.

We then used the crystal structure of G$\beta_1\gamma_2$ from the structure of the GRK2-G$\beta_1\gamma_2$ complex (PDB entry 1OMW)[43] to predict the expected amide I net molecular responses from helical portions of the protein (see Supporting Information), for comparison with the measured parameters $\chi^{(2)}_{zzz}/\chi^{(2)}_{xxz}$ (from SFG measurements) and the dichroic ratio R^{ATR} (from ATR-FTIR spectroscopy). The structure of G$\beta\gamma$ does not change significantly when in complex with any of the targets that has been characterized thus far (GRK2, Gα, phosducin, SIGK peptide). We chose the 1OMW structure of G$\beta_1\gamma_2$ (GRK2-bound) simply because its extended N-terminal helices were not involved in crystal contacts as they are in other crystal forms, and thus this structure is more likely to represent the conformation of G$\beta\gamma$ in solution. SFG observable quantities were calculated for all unique orientations of the heterodimer relative to the reference orientation shown in Figure 1. As shown in Figure 3A, many possible twist and tilt angle combinations produce the experimentally determined $\chi^{(2)}_{zzz}/\chi^{(2)}_{xxz}$ ratio of 2.0 ± 0.2, indicating once again that the SFG measurement alone cannot determine a single unique orientation of G$\beta_1\gamma_2$. Figure 3B shows orientations that would generate an ATR-FTIR dichroic ratio of 1.7 ± 0.2. Again, many combinations of twist and tilt angle are possible, but they are distinct from matches for the SFG measurement

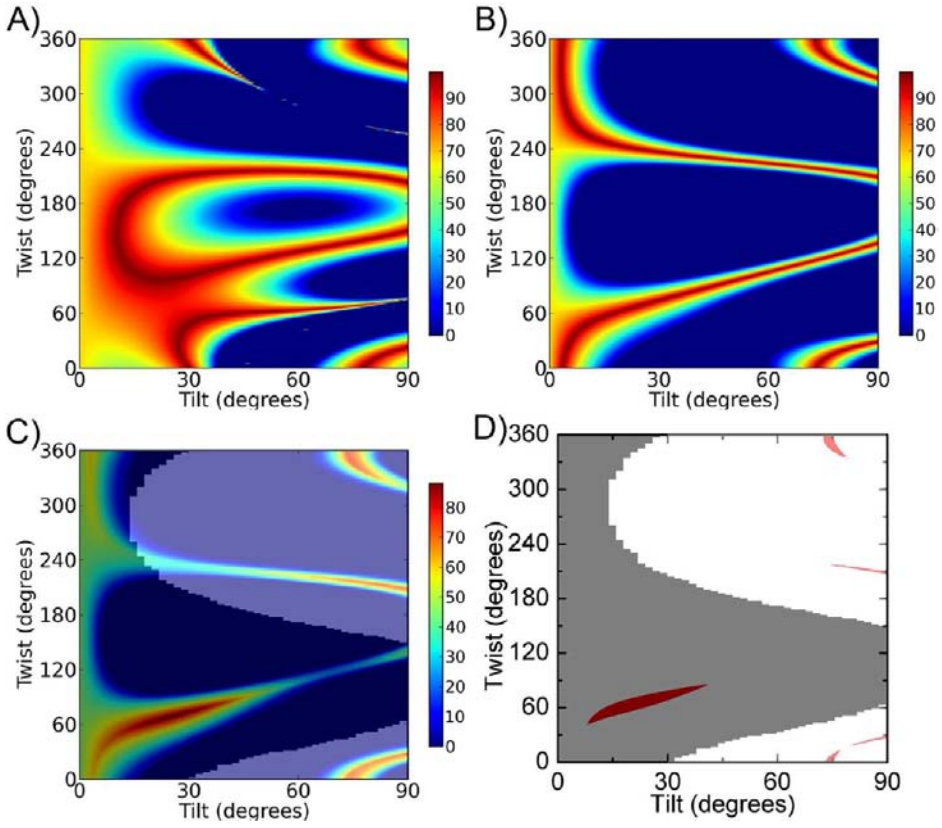

Figure 3. The possible orientations of G$\beta_1\gamma_2$ determined by (A) SFG ($\chi^{(2)}_{zzz}/\chi^{(2)}_{xxz}$ = 2.0 ± 0.2), (B) ATR-FTIR (dichroic ratio R^{ATR} =1.7 ± 0.2), and (C) the combination of SFG and ATR-FTIR measurements. The effect of experimental errors (such as uncertainty in the Fresnel coefficients) is accounted for using a coloring scheme based on how well the calculated and experimentally measured quantities agree for each possible orientation, within specified error bars (±10%).[41] If the calculated $\chi^{(2)}_{zzz}/\chi^{(2)}_{xxz}$ ratio does not match the experimental value within ±10%, a score of 0 is assigned. In panel C, the total score is calculated as the product of the scores for all individual criteria. A score of 100% indicates an exact match for all experimental measurements. The shaded areas indicate orientations of G$\beta_1\gamma_2$ that are considered to be physically reasonable, according to previously defined criteria.[41] (D) The possible orientation areas with a score ≥70% (red).

dx.doi.org/10.1021/ja3116026 | J. Am. Chem. Soc. 2013, 135, 5044−5051

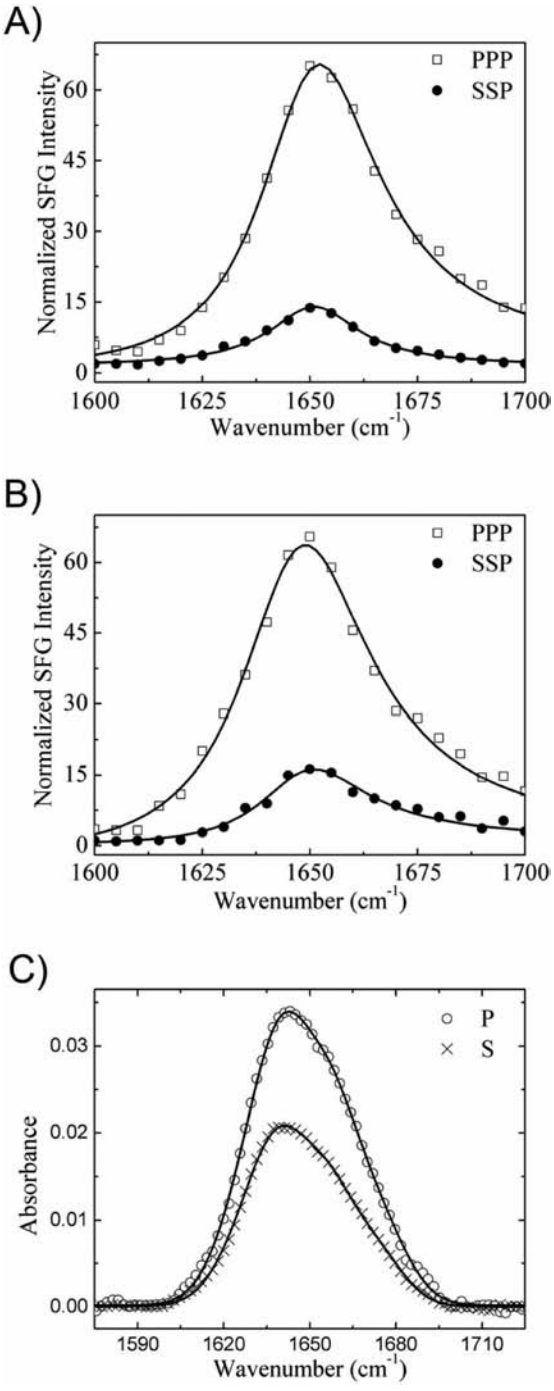

Figure 4. SFG Amide I region signals from (A) 336 nM $G\alpha_i\beta_1\gamma_2$ heterotrimer or (B) myr-$G\alpha_i\beta_1\gamma_2$ heterotrimer interacting with a 9:1 POPC:POPG lipid bilayer. (C) ATR-FTIR Amide I region signals from 336 nM $G\alpha_i\beta_1\gamma_2$ heterotrimer interacting with a 9:1 POPC:POPG lipid bilayer. The squares, circles, and crosses are experimental data. The solid lines are the fitting results.

(Figure 3A). Thus, combining the available orientations determined by the ATR-FTIR dichroic ratio R^{ATR} with constraints from the SFG $\chi^{(2)}_{zzz}/\chi^{(2)}_{xxz}$ ratio yields a much narrower range of possible orientations of $G\beta_1\gamma_2$ (Figures 3C and 3D), which fall in a narrow range of moderate twist angles (50−80°) and low tilt angles (15−35°). Additional arcs of matches exist for $G\beta_1\gamma_2$ at high tilt angles ∼75°, but such positions would place the geranylgeranyl group quite far from the bilayer and are therefore physically unlikely. The combination of SFG and ATR-FTIR measurements points to a single favored orientation range for $G\beta_1\gamma_2$ on the lipid bilayer *in situ*. All orientations in this range correspond to closely related configurations where the C-terminus of $G\gamma_2$ would be in close proximity to the membrane, consistent with the geranylgeranyl group being the dominant membrane binding determinant of $G\beta_1\gamma_2$.

Orientation of $G\alpha_i\beta_1\gamma_2$. Although $G\alpha_i$ is N-terminally myristoylated in cells, we first chose to examine the effect of nonmyristoylated $G\alpha_i$ on complex formation $G\beta\gamma$ to avoid the complication of spectroscopic signals originating from membrane bound $G\alpha_i$ in addition to those from a reconstituted $G\alpha_i\beta_1\gamma_2$ heterotrimer. Indeed, no SFG signals could be detected from nonmyristoylated $G\alpha_i$ alone (data not shown). However, SFG amide I signal could be readily detected for the $G\alpha_i\beta_1\gamma_2$ heterotrimer (Figure 4A) and exhibited strong contributions from α-helices centered at 1652 cm^{-1}. SFG spectra for a preformed $G\alpha_i\beta_1\gamma_2$ heterotrimer were identical to those obtained by adding the two subunits to the lipid bilayer subphase sequentially (first $G\beta_1\gamma_2$, followed by $G\alpha_i$), but distinct from the spectra of $G\beta_1\gamma_2$ alone,[41] demonstrating that the $G\alpha_i\beta_1\gamma_2$ heterotrimer can be formed at the membrane *in situ* in our experiments. It was found that the measured ratio $\chi^{(2)}_{zzz}/\chi^{(2)}_{xxz}$ for the α-helical peak centered at 1652 cm^{-1} was 2.67. Possible values of $\chi^{(2)}_{zzz}/\chi^{(2)}_{xxz}$ for various orientations of $G\alpha_i\beta_1\gamma_2$ were calculated (see Supporting Information) based on a modified structure of the $G\alpha_i\beta_1\gamma_2$ heterotrimer (PDB entry 1GP2)[80] in which the structure of the $G\beta_1\gamma_2$ portion was taken from a structure of GRK2-$G\beta_1\gamma_2$ (PDB entry 1OMW)[43] for the reasons described above. The calculated and experimentally determined orientation parameters were compared, yielding possible orientations of $G\alpha_i\beta_1\gamma_2$ (Figure 5A). Once again, the SFG results alone were insufficient to uniquely determine the overall orientation of the protein.

ATR-FTIR spectra were also collected for $G\alpha_i\beta_1\gamma_2$ (Figure 4C), and the calculated relationship between dichroic ratio R^{ATR} and heterotrimer orientation (Supporting Information) was compared to the experimentally measured value of R^{ATR} = 1.75 based on the α-helical peak center at 1657 cm^{-1} (see Supporting Information). The broad range of possible matches for the ATR-FTIR measurement is shown in Figure 5C, and the greatly narrowed range of matches obtained by combining ATR-FTIR and SFG measurements is shown in Figures 5D and 5E. The best matches fall in a very narrow range of moderate twist angles (∼65°) and low tilt angles (∼23°), with some additional matches at high tilt angles (75−85°) that can be rejected as physically unlikely. Thus, the combination of SFG and ATR-FTIR spectroscopy makes it possible to determine the orientation of $G\alpha_i\beta_1\gamma_2$ more precisely than using either technique alone.

To ensure that the myristoyl group has no impact on the membrane orientation of $G\alpha_i\beta_1\gamma_2$, we also collected SFG spectra from samples of the myr-$G\alpha_i\beta_1\gamma_2$ heterotrimer. SFG amide I signals could be detected (Figure 4B) with strong contributions from α-helices centered at 1652 cm^{-1}. The spectral features detected from the myr-$G\alpha_i\beta_1\gamma_2$ heterotrimer (Figure 4B) were very similar to those from the nonmyristoylated $G\alpha_i\beta_1\gamma_2$ heterotrimer (Figure 4A). The measured ratio $\chi^{(2)}_{zzz}/\chi^{(2)}_{xxz}$ for the α-helical peak centered at 1652 cm^{-1} was determined to be 2.51, very close to the value of $G\alpha_i\beta_1\gamma_2$ heterotrimer (2.67). Making the reasonable assumption that the structure of $G\alpha_i\beta_1\gamma_2$ is unaffected by the myristoyl group, we were able to calculate the expected SFG observables, and

dx.doi.org/10.1021/ja3116026 | J. Am. Chem. Soc. 2013, 135, 5044−5051

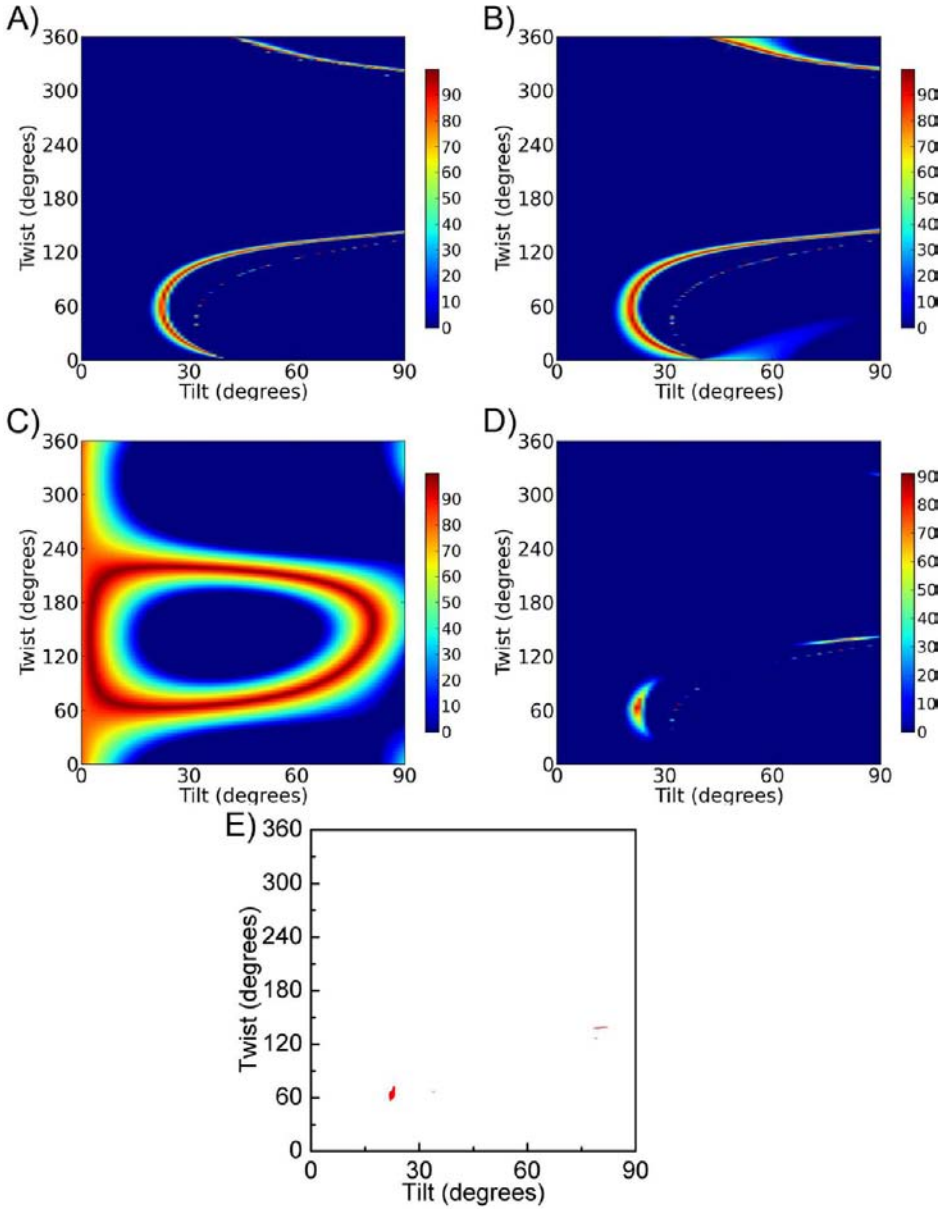

Figure 5. The possible orientations of G$\alpha_i\beta_1\gamma_2$ determined by (A) the SFG ratio of $\chi^{(2)}_{zzz}/\chi^{(2)}_{xxz}$ (2.7 ± 0.3) and the possible orientations of myr-G$\alpha_i\beta_1\gamma_2$ determined by (B) the SFG ratio of $\chi^{(2)}_{zzz}/\chi^{(2)}_{xxz}$ (2.5 ± 0.3). Orientations of G$\alpha_i\beta_1\gamma_2$ at which the calculated values best match experimentally measured values for (C) the ATR-FTIR dichroic ratio R^{ATR} (1.8 ± 0.2). The product of these two measurements of G$\alpha_i\beta_1\gamma_2$ (D) further narrows the range of possible orientations. (E) Same plot as panel D but only showing orientation areas with a score ≥70% (red).

found a similar range of possible orientations for myr-G$\alpha_i\beta_1\gamma_2$ (Figure 5B) as for G$\alpha_i\beta_1\gamma_2$ (Figure 5A). This suggests that the myristoyl group does not substantially impact the orientation of G$\alpha_i\beta_1\gamma_2$, consistent with the fact that the myristoyl group is predicted to be in close proximity to the geranylgeranyl group of Gγ_2 in the complex, and both modifications occur on flexible regions of their respective proteins.

Comparison of the Orientation of G$\beta_1\gamma_2$ Alone and in Complex with Gα_i. Comparison of the most likely orientations for G$\beta_1\gamma_2$ (Figure 3C) and G$\alpha_i\beta_1\gamma_2$ (Figure 5D) reveals that there is substantial overlap between the two plots, suggesting that it is possible for the G$\alpha_i\beta_1\gamma_2$ heterotrimer to form without reorientation of G$\beta_1\gamma_2$. To consider the possibility of a common orientation more quantitatively, we directly combined all four available measurements (two $\chi^{(2)}_{zzz}/\chi^{(2)}_{xxz}$ ratios and two dichroic R^{ATR} ratios) in one plot, thereby testing the assumption that G$\beta_1\gamma_2$ and G$\alpha_i\beta_1\gamma_2$ adopt the same orientation. Figure 6A shows the orientations of both G$\beta_1\gamma_2$ *and* the G$\alpha_i\beta_1\gamma_2$ heterotrimer that would satisfy all of the SFG and ATR-FTIR measurements. The most likely orientation range has twist from 50 to 80° and low tilt angles from 20 to 25°, with an assigned score of 68% at ψ = 67°, θ = 23°. Because overall scores are the product of scores for all individual measurements, this indicates that all individual criteria would provide good quality matches between experimental and calculated parameters ($\sim(67\%)^{1/4}$ = 90% or better). Thus, it is reasonable to assume that G$\beta_1\gamma_2$ does not reorient upon formation of the heterotrimer. A proposed shared orientation for G$\beta_1\gamma_2$ and G$\alpha_i\beta_1\gamma_2$ is shown in Figure 7. In this pose, the orientation of G$\beta\gamma$ at the membrane would allow association with GDP-bound inactive Gα subunits in a manner that would not create an overlap between Gα and the membrane plane. Furthermore,

dx.doi.org/10.1021/ja3116026 | J. Am. Chem. Soc. 2013, 135, 5044−5051

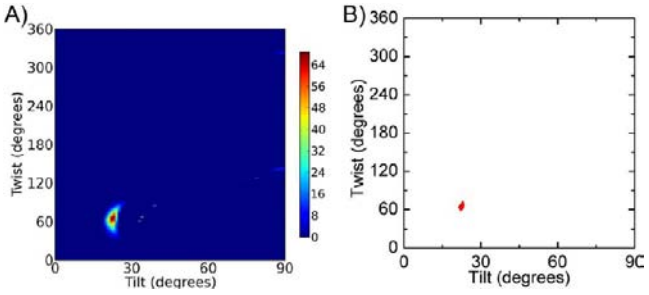

Figure 6. Assessment of whether the $G\beta_1\gamma_2$ subunit and $G\alpha_i\beta_1\gamma_2$ can adopt similar orientations at the membrane. (A) Scores for orientations that satisfy all four measurements (two $\chi^{(2)}_{zzz}/\chi^{(2)}_{xxz}$ ratios and two dichroic R^{ATR} ratios). These scores would represent good matches for all experimentally measured parameters, and suggests that $G\beta_1\gamma_2$ does not greatly change its orientation when bound to $G\alpha_i$. (B) The same plot as panel A but only showing the orientation area with a score ≥50% (red).

the relatively static orientation of $G\beta_1\gamma_2$ at the membrane allows for the disassociation from a complex with $G\alpha$ and rapid association with other signaling molecules, such as GRK2. These results also indicate that the amino acid sequence of $G\alpha$ does not contain regions that strongly influence the membrane orientation of the $G\alpha\beta\gamma$ heterotrimer, consistent with the lack of SFG signals obtained for nonmyristoylated $G\alpha_i$. Thus, this deduced orientation may be exhibited by all families of heterotrimeric G proteins.

CONCLUSIONS

In this work, we combined SFG and ATR-FTIR to determine the membrane orientation of $G\beta_1\gamma_2$ and the $G\alpha_i\beta_1\gamma_2$ heterotrimer *in situ*. SFG and ATR-FTIR vibrational spectroscopies measure complementary independent parameters, and the combination of techniques was shown to provide a more precise orientation than could be obtained using either technique alone. The most likely orientations of $G\beta_1\gamma_2$ fall in a range of moderate twist angles (50−80°) and low tilt angles (15−35°), whereas the most likely orientation of the $G\alpha_i\beta_1\gamma_2$ heterotrimer falls in a very narrow range of moderate twist angles (~65°) and low tilt angles (~23°). According to our measurements, it is entirely possible that $G\beta_1\gamma_2$ can bind to $G\alpha_i$ without changing its orientation (twist = 67°, tilt = 23°) relative to the lipid bilayer. In this orientation (Figure 7), the parts of the protein closest to the lipid bilayer are the C-terminus of $G\gamma_2$ and basic residues at the extreme N-terminus of $G\alpha_i$ (which are conserved among all $G\alpha$ subunits). Our analysis of the myr-$G\alpha_i\beta_1\gamma_2$ complex indicated that the myristoyl group does not strongly dictate the orientation of the heterotrimeric G protein complex ($G\alpha\beta\gamma$), in which the $G\beta_1\gamma_2$ subunits do not undergo a large conformational change in response to binding the $G\alpha_i$. This could be due to close proximity of the lipid modifications in the complex (N-terminus of $G\alpha_i$ and C-terminus of $G\beta_1\gamma_2$) to each other and on flexible regions of the protein or due to the longer geranylgeranylation modification of $G\beta_1\gamma_2$ which likely dominates the membrane localization of the heterotrimeric G protein complex compared to the shorter myristoyl chain of $G\alpha$.

A low-resolution structure of transducin ($G\alpha_t\beta_1\gamma_1$) bound to PC lipid tubules was previously determined in helical reconstructions from cryo electron micrographs.[81] This work suggested that the heterotrimer binds to the tubules via two strong contacts, which were modeled as the N-terminus and C-terminus of the $G\alpha_t$ subunit, the former of which presumably included the farnesylated C-terminus of $G\gamma_1$. Their proposed membrane orientation is significantly different than that suggested in our study (Figure 7) because it suggests that the C-terminus of transducin is involved in membrane binding, whereas we find no evidence that regions other than the extreme N-terminus of $G\alpha_i$ are involved. The conflicting results could reflect several experimental differences. The first could be the influence of helical crystal contacts on the orientation of the transducin-lipid tubule complex in the EM study. Furthermore, although close homologues, the proteins involved in the two studies were distinct, and $G\gamma_1$ is farnesylated instead of geranylgeranylated like $G\gamma_2$. Finally, there were differences in the composition of the lipid environment used in each study. Whereas the electron microscopy study used neutral lipids, we used a 9:1 mix of POPC and POPG lipids that more closely reflects the charge of the inner leaflet of the membrane surface. In future studies it will be interesting to examine the effect of a change in lipid composition on the orientation of heterotrimeric G proteins and their complexes.

The observation that $G\beta_1\gamma_2$ does not seem to change its orientation significantly as it engages $G\alpha_i$ suggests that the geranylgeranyl modification of $G\gamma_2$ is most important determinant of the orientation of $G\alpha_i\beta_1\gamma_2$ in membranes, at least in the context of the model phospholipid bilayer we employed. Other regions of the heterotrimer do not lie in the plane of the membrane, such as the C-terminus of $G\alpha$, which forms the primary contact with activated integral membrane GPCRs (our model system contains lipids, but not GPCRs).[37] Thus, when the heterotrimer encounters an activated GPCR, it will need to change its membrane orientation as a result of

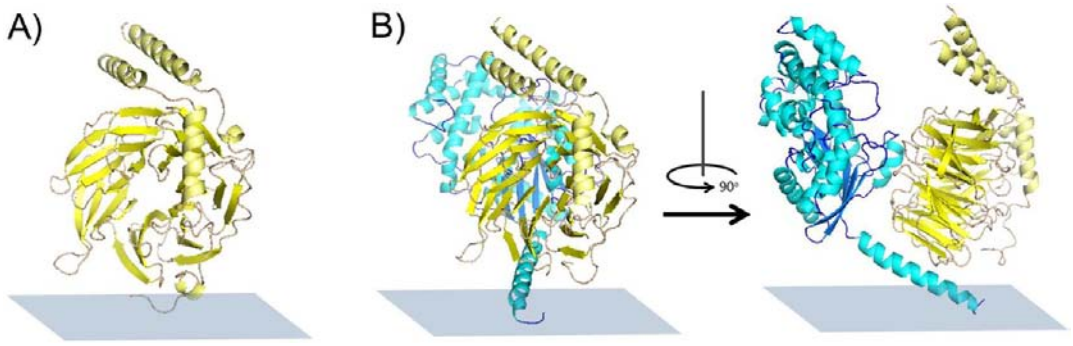

Figure 7. Possible membrane orientation of (A) $G\beta_1\gamma_2$, and (B) $G\alpha_i\beta_1\gamma_2$ as determined from our experimental measurements (twist = 67°, tilt = 23°). Two views related by 90° are shown. The plane of the membrane relative to the protein is shown as a blue rectangle.

dx.doi.org/10.1021/ja3116026 | J. Am. Chem. Soc. 2013, 135, 5044−5051

additional strong interactions created between the receptor and Gα. The "basal" orientations of G$\beta_1\gamma_2$ and the G$\alpha_i\beta_1\gamma_2$ determined in this work may be of physiological relevance because they allow unhindered access to the protein-interaction surfaces of each complex (i.e., the Gα-binding face of the β-propeller of Gβ_1 and the C-terminus and other regions of Gα that interact with GPCRs). For example, a previous study showed that altering the location of the prenylation site in Gγ_5 by deleting 10 residues immediately N-terminal to the modified cysteine (Gγ_5-Δ55−64) abrogates the ability of G$\beta\gamma_5$-Δ55−64 to activate the effector enzyme phospholipase Cβ.[82] Although there are other possible explanations,[82] it is tempting to speculate that this phenotype at least in part reflects a change in the orientation of G$\beta\gamma_5$-Δ55−64 at the membrane that either makes it more difficult for phospholipase Cβ to access its binding site on G$\beta\gamma$, or constrains the resulting complex into an orientation that is not optimal for phospholipid hydrolysis.

It could be argued that the proteins we studied adopt a different conformation upon interacting with membranes, which would limit the usefulness of crystal structures to serve as models for our calculations. However, both G$\beta_1\gamma_2$ and Gα_iG$\beta_1\gamma_2$ interact with membranes primarily through lipid-modified regions that are intrinsically disordered. Because these regions are not coupled to the core structure of the complex, it seems unlikely that their interaction with membrane will induce a large conformational change. Thus, we are comfortable with the required assumption that G$\beta_1\gamma_2$ and Gα_i do not undergo large conformational changes upon protein−protein interactions and membrane binding, as suggested by comparison of their various crystal structures.

We believe that the combination of SFG and ATR-FTIR will provide a foundation for future studies on larger protein complexes, and will enable studies of how each component affects the overall orientation of the complex in order to accommodate additional binding partners. With the help of other advanced approaches currently being developed (e.g., isotope labeling), we believe that in the future it will be possible to deduce an even more accurate orientation for a large protein complex using combined vibrational spectroscopic studies.

■ ASSOCIATED CONTENT

Supporting Information

Details of the theory and orientation analysis methodologies relevant to SFG and ATR-FTIR, as well as additional information about spectral fitting results for ATR-FTIR. This material is available free of charge via the Internet at http://pubs.acs.org.

■ AUTHOR INFORMATION

Corresponding Author

zhanc@umich.edu; tesmerjj@umich.edu

Notes

The authors declare no competing financial interest.

■ ACKNOWLEDGMENTS

We thank Mark R. Nance, Dr. Valerie Tesmer, and Tracy Quay for technical assistance, and Bei Ding for insightful discussion. This work was supported by NIH grant GM081655 to Z.C. and J.J.G.T., and by NIH grants HL071818 and HL086865 (to J.J.G.T.).

■ REFERENCES

(1) Horbett, T. A.; Brash, J. L. *Proteins at Interfaces II: Fundamentals and Applications (ACS Symposium)*; American Chemical Society: Washington, DC, 1995.
(2) Giangaspero, A.; Sandri, L.; Tossi, A. *Eur. J. Biochem.* **2001**, *268*, 5589−5600.
(3) Morris, M. C.; Deshayes, S.; Heitz, F.; Divita, G. *Biol. Cell* **2008**, *100*, 201−217.
(4) Tweedle, M. F. *Acc. Chem. Res.* **2009**, *42*, 958−968.
(5) Chen, H.; Xu, Z.; Peng, L.; Fang, X.; Yin, X.; Xu, N.; Cen, P. *Peptides* **2006**, *27*, 931−940.
(6) Jin, W. *Anal. Chim. Acta* **2002**, *461*, 1−36.
(7) Benkovic, S. J.; Hammes-Schiffer, S. *Science* **2003**, *301*, 1196−1202.
(8) Grozea, C. M.; Walker, G. C. *Soft Matter* **2009**, *5*, 4088−4100.
(9) Nguyen, K.; Le Clair, S.; Ye, S.; Chen, Z. *J. Phys. Chem. B* **2009**, *113*, 12169−12180.
(10) Wang, J.; Lee, S. −H.; Chen, Z. *J. Phys. Chem. B* **2008**, *112*, 2281−2290.
(11) Wang, J.; Chen, X.; Clarke, M. L.; Chen, Z. *Proc. Natl. Acad. Sci. U.S.A.* **2005**, *102*, 4978−4983.
(12) Nguyen, K.; King, J. T.; Chen, Z. *J. Phys. Chem. B* **2010**, *114*, 8291−8300.
(13) Yang, P.; Ramamoorthy, A.; Chen, Z. *Langmuir* **2011**, *27*, 7760−7767.
(14) Ye, S.; Li, H.; Wei, F.; Jasensky, J.; Boughton, A. P.; Yang, P.; Chen, Z. *J. Am. Chem. Soc.* **2012**, *134*, 6237−6243.
(15) Wang, T.; Li, D.; Lu, X.; Khmaladze, A.; Han, X.; Ye, S.; Yang, P.; Xu, G.; He, N.; Chen, Z. *J. Phys. Chem. C* **2011**, *115*, 7613−7620.
(16) Thennarasu, S.; Huang, R.; Lee, D. K.; Yang, P.; Maloy, L.; Chen, Z.; Ramamoorthy, A. *Biochemistry* **2010**, *49*, 10595−10605.
(17) Ding, B.; Chen, Z. *J. Phys. Chem. B* **2012**, *116*, 2545−2552.
(18) Ye, S.; Nguyen, K.; Chen, Z. *J. Phys. Chem. B* **2010**, *114*, 3334−3340.
(19) Han, X.; Soblosky, L.; Slutsky, M.; Mello, C. M.; Chen, Z. *Langmuir* **2011**, *27*, 7042−7051.
(20) Ye, S.; Nguyen, K.; Boughton, A. P.; Mello, C. M.; Chen, Z. *Langmuir* **2010**, *26*, 6471−6477.
(21) Clarke, M. L.; Wang, J.; Chen, Z. *J. Phys. Chem. B* **2005**, *109*, 22027−22035.
(22) Nguyen, K.; Soong, R.; Im, S.; Waskell, L.; Ramamoorthy, A.; Chen, Z. *J. Am. Chem. Soc.* **2010**, *132*, 15112−15115.
(23) Chen, X.; Wang, J.; Boughton, A. P.; Kristalyn, C. B.; Chen, Z. *J. Am. Chem. Soc.* **2007**, *129*, 1420−1427.
(24) Wang, J.; Paszti, Z.; Clarke, M. L.; Chen, X.; Chen, Z. *J. Phys. Chem. B* **2007**, *111*, 6088−6095.
(25) Nguyen, K. T.; Le Clair, S. V.; Ye, S.; Chen, Z. *J. Phys. Chem. B* **2009**, *113*, 12358−12363.
(26) Frey, S.; Tamm, L., K. *Biophys. J.* **1991**, *60*, 922−930.
(27) Tamm, L., K.; Tatulian, S., A. *Q. Rev. Biophys.* **1997**, *30*, 365−429.
(28) Marsh, D. *J. Mol. Biol.* **2004**, *338*, 353−367.
(29) Marsh, D. *Biophys. J.* **1997**, *72*, 2710−2718.
(30) Páli, T.; Marsh, D. *Biophys. J.* **2001**, *80*, 2789−2797.
(31) Ramakrishnan, M.; Qu, J.; Pocanschi, C. L.; Kleinschmidt, J. H.; Marsh, D. *Biochemistry* **2005**, *44*, 3515−3523.
(32) Rodionova, N. A.; Tatulian, S. A.; Surrey, T.; Jaehnig, F.; Tamm, L. K. *Biochemistry* **1995**, *34*, 1921−1929.
(33) Gray, C.; Tamm, L. K. *Protein Sci.* **1997**, *6*, 1993−2006.
(34) Tatulian, S. A.; Hinterdorfer, P.; Baber, G.; Tamm, L. K. *EMBO J.* **1995**, *14*, 5514−5523.
(35) Lodowski, D. T.; Barnhill, J. F.; Pitcher, J. A.; Capel, W. D.; Lefkowitz, R. J.; Tesmer, J. J. G. *Acta Crystallogr., Sec. D: Biol. Crystallogr.* **2003**, *59*, 936−939.
(36) Neves, S. R.; Ram, P. T.; Iyengaar, R. *Science* **2002**, *296*, 1636−1639.
(37) Rasmussen, S. G.; DeVree, B. T.; Zou, Y.; Kruse, A. C.; Chung, K. Y.; Kobilka, T. S.; Thian, F. S.; Chae, P. S.; Pardon, E.; Calinski, D.; Mathiesen, J. M.; Shah, S. T.; Lyons, J. A.; Caffrey, M.; Gellman, S. H.;

Steyaert, J.; Skiniotis, G.; Weis, W. I.; Sunahara, R. K.; Kobilka, B. K. *Nature* **2011**, *477*, 549−555.
(38) Tesmer, V. M.; Kawano, T.; Shankaranarayanan, A.; Kozasa, T.; Tesmer, J. J. G. *Science* **2005**, *310*, 1686−1690.
(39) Wood, J. F.; Wang, J.; Benovic, J. L.; Ferkey, D. M. *J. Biol. Chem.* **2012**, *287*, 12634−12644.
(40) Evron, T.; Daigle, T. L.; Caron, M. G. *Trends Pharmacol. Sci.* **2012**, *33*, 154−164.
(41) Boughton, A. P.; Yang, P.; Tesmer, V. M.; Ding, B.; Tesmer, J. J.; Chen, Z. *Proc. Natl. Acad. Sci. U.S.A.* **2011**, *108*, E667−E673.
(42) Linder, M. E.; Gilman, A. G. *Methods Enzymol.* **1991**, *195*, 202−215.
(43) Lodowski, D. T.; Pitcher, J. A.; Capel, W. D.; Lefkowitz, R. J.; Tesmer, J. J. G. *Science* **2003**, *300*, 1256−1262.
(44) Chen, X.; Boughton, A. P.; Tesmer, J. J. G.; Chen, Z. *J. Am. Chem. Soc.* **2007**, *129*, 12658−12659.
(45) Yang, P.; Wu, F. G.; Chen, Z. *J. Phys. Chem C* **2013**, *117*, 3358−3365.
(46) Wang, J.; Even, M. A.; Chen, X.; Schmaier, A. H.; Waite, J. H.; Chen, Z. *J. Am. Chem. Soc.* **2003**, *125*, 9914−9915.
(47) Shen, Y., R. *Nature* **1989**, *337*, 519−525.
(48) Eisenthal, K. B. *Chem. Rev.* **1996**, *96*, 1343−1360.
(49) Kim, J.; Somorjai, G. A. *J. Am. Chem. Soc.* **2003**, *125*, 3150−3158.
(50) Richmond, G. L. *Chem. Rev.* **2002**, *102*, 2693−2724.
(51) Kim, J.; Cremer, P. S. *Chem. Phys. Chem* **2001**, *2*, 543−546.
(52) Wang, H.; Gang, W.; Lu, R.; Rao, Y.; Wu, B. *Int. Rev. Phys. Chem.* **2005**, *24*, 191−256.
(53) Bain, C. D. *J. Chem. Soc., Dalton Trans.* **1995**, *91*, 1281−1296.
(54) Haupert, L. M.; Simpson, G. J. *Annu. Rev. Phys. Chem.* **2009**, *60*, 345−365.
(55) Liljeblad, J. F. D.; Bulone, V.; Rutland, M. W.; Johnson, C. M. *J. Phys. Chem C* **2011**, *115*, 10617−10629.
(56) Li, G.; Ye, S.; Morita, S.; Nishida, T.; Osawa, M. *J. Am. Chem. Soc.* **2004**, *126*, 12198−12199.
(57) Barth, C.; Jakubczyk, D.; Kubas, A.; Anastassacos, F.; Brenner-Weiss, G.; Fink, K.; Schepers, U.; Brase, S.; Koelsch, P. *Langmuir* **2012**, *28*, 8456−8462.
(58) Engelhardt, K.; Rumpel, A.; Walter, J.; Dombrowski, J.; Kulozik, U.; Braunschweig, B.; Peukert, W. *Langmuir* **2012**, *28*, 7780−7787.
(59) Liu, J.; Conboy, J. C. *J. Am. Chem. Soc.* **2004**, *126*, 8894−8895.
(60) Ye, S.; Liu, G.; Li, H.; Chen, F.; Wang, X. *Langmuir* **2012**, *28*, 1374−1380.
(61) Ma, G.; Liu, D. F.; Allen, H. C. *Langmuir* **2004**, *20*, 11620−11629.
(62) Weidner, T.; Breen, N. F.; Li, K.; Drohny, G. P.; Castner, D. G. *Proc. Natl. Acad. Sci. U.S.A.* **2010**, *107*, 13288−13293.
(63) Weidner, T.; Breen, N. F.; Drobny, G. P.; Castner, D. G. *J. Phys. Chem. B* **2009**, *113*, 15423−15426.
(64) Weidner, T.; Dubey, M.; Breen, N. F.; Ash, J.; Baio, J. E.; Jaye, C.; Fischer, D. A.; Drobny, G. P.; Castner, D. G. *J. Am. Chem. Soc.* **2012**, *134*, 8750−8753.
(65) Fu, L.; Ma, G.; Yan, E. C. *J. Am. Chem. Soc.* **2010**, *132*, 5405−5412.
(66) Fu, L.; Liu, J.; Yan, E. C. *J. Am. Chem. Soc.* **2011**, *122*, 8094−8097.
(67) Chen, X.; Flores, S. C.; Lim, S. M.; Zhang, Y. J.; Yang, T. L.; Kherb, J.; Cremer, P. S. *Langmuir* **2010**, *26*, 16447−16454.
(68) Campen, R. K.; Ngo, T. T. M.; Sovago, M.; Ruysschaert, J. M.; Bonn, M. *J. Am. Chem. Soc.* **2010**, *132*, 8037−8047.
(69) Wang, H. F.; Troxler, T.; Yeh, A. G.; Dai, H. L. *J. Phys. Chem. C* **2007**, *111*, 8708−8715.
(70) Jen, S. H.; Dai, H. L. *J. Phys. Chem. B* **2006**, *110*, 23000−23003.
(71) Ye, H.; Abu-Akeel, A.; Huang, J.; Katz, H. E.; Gracias, D. H. *J. Am. Chem. Soc.* **2006**, *128*, 6528−6529.
(72) Ye, H.; Gu, Z.; Gracias, D. H. *Langmuir* **2006**, *22*, 1863−1868.
(73) Ye, H.; Huang, J.; Park, J. R.; Katz, H. E.; Gracias, D. H. *J. Phys. Chem. C* **2007**, *111*, 13250−13255.
(74) Li, Q.; Kuo, C. W.; Yang, Z.; Chen, P.; Chou, K. C. *Phys. Chem. Chem. Phys.* **2009**, *11*, 3436−3442.
(75) Chen, P.; Kung, K. Y.; Shen, Y. R.; Somorjai, G. A. *Surf. Sci.* **2001**, *494*, 289−297.
(76) Leung, B. O.; Yang, Z.; Wu, S. S. H.; Chou, K. C. *Langmuir* **2012**, *28*, 5724−5728.
(77) Yang, Z.; Li, Q.; Gray, M. R.; Chou, K. C. *Langmuir* **2010**, *26*, 16397−16400.
(78) Chen, X.; Yang, T.; Kataoka, S.; Cremer, P. S. *J. Am. Chem. Soc.* **2007**, *129*, 12272−12279.
(79) Tatulian, S. A.; Jones, L. R.; Reddy, L. G.; Stokes, D. L.; Tamm, L. K. *Biochemistry* **1995**, *34*, 4448−4456.
(80) Wall, M. A.; Coleman, D. E.; Lee, E.; Iniguez-Lluhi, J. A.; Posner, B. A.; Gilman, A. G.; Sprang, S. R. *Cell* **1995**, *83*, 1047−1058.
(81) Zhang, Z.; Melia, T. J.; He, F.; Yuan, C.; Mcgough, A.; Schmid, M. F.; Wensel, T. G. *J. Biol. Chem.* **2004**, *279*, 33937−33945.
(82) Akgoz, M.; Azpiazu, I.; Kalyanaraman, V.; Gautam, N. *J. Biol. Chem.* **2002**, *277*, 19573−19578.